

Controlled Self-Assembly of Asymmetric Dumbbell-Shaped Rod Amphiphiles: Transition from Toroids to Planar Nets

Eunji Lee, Young-Hwan Jeong, Jung-Keun Kim, and Myongsoo Lee*

Center for Supramolecular Nano-Assembly and Department of Chemistry, Yonsei University, Seoul 120-749, Korea

Received July 9, 2007; Revised Manuscript Received September 3, 2007

ABSTRACT: We report here the synthesis and self-assembly of a series of asymmetric dumbbell-shaped rod amphiphiles containing hydrophilic oligoether dendrons at one end and hydrophobic alkyl dendrons at the other end of the stiff rod segment with systematic variation in the length of the hydrophobic alkyl chain ranging from ethyl to tetradecyl groups. These rod amphiphiles were observed to self-assemble, in aqueous solution, into nanoscopic supramolecular aggregates that change significantly on variation in the length of hydrophobic alkyl chain, as characterized by cryo-transmission electron microscopy (cryo-TEM) experiments. The rod amphiphile based on the ethyl group ($f_{\text{alkyl/EO}} = 0.45$) exhibits a spherical micellar structure, while the amphiphile with the hexyl group ($f_{\text{alkyl/EO}} = 0.71$) shows a toroidal structure. Further increasing the alkyl length to decyl ($f_{\text{alkyl/EO}} = 0.97$) and tetradecyl ($f_{\text{alkyl/EO}} = 1.23$) gives rise to the formation of two-dimensional networks and vesicles, respectively. Remarkably, the toroidal structure showed to change into two-dimensional networks on heating in a reversible way due to a lower critical solution temperature (LCST) behavior of the oligoether dendritic exterior. This structural change takes place directly without passing through any intermediate structures. The results described here demonstrate that systematic variation in the hydrophobic chain length of the rod amphiphiles can provide access to a wide variety of self-assembled nanostructures in aqueous solution. The primary driving force for this unique self-assembling behavior is proposed to be the energy balance between repulsive interactions of the hydrophilic oligoether dendrons and attractive hydrophobic interactions of the rod segments.

Introduction

Manipulation of supramolecular nanostructure in self-organizing materials is of paramount importance in achieving desirable functions and properties, which has great potential implication both fundamentally and practically in the fields of chemical biology and material science.¹ In particular, amphiphilic molecular architecture containing a rigid rod segment can give rise to well-defined nanoscopic structures including bundles, ribbons, tubules, and vesicles in solution.² These self-assembled architectures can be manipulated by the precise control of molecular structure such as the type and relative length of the respective blocks.³ For example, incorporation of flexible chains into both ends of a rigid segment leads to the formation of 1-D cylindrical objects in a selective solvent for flexible chains.⁴ In addition, amphiphilic rod derivatives substituted with flexible chiral chains self-assemble into 1-D objects with a preferred-handed supramolecular helicity.⁵ We have also shown that symmetric dumbbell-shaped amphiphilic molecules consisting of conjugated aromatic rod and chiral aliphatic polyether dendrons, in aqueous solution, result in the formation of helical nanofibers in which the rod segments stack on top of each other with mutual rotation.^{6,7} The helical fibers, on addition of hydrophobic guest molecules, transform into a hollow capsulelike structure. This dynamic structural variation is attributed to the packing change of the rod segment from a twisted to a parallel arrangement caused by the energy balance between repulsive interactions among the adjacent hydrophilic dendritic chain and attractive π -stacking interactions. Replacement of one of the hydrophilic dendrons into a hydrophobic one produces asymmetric molec-

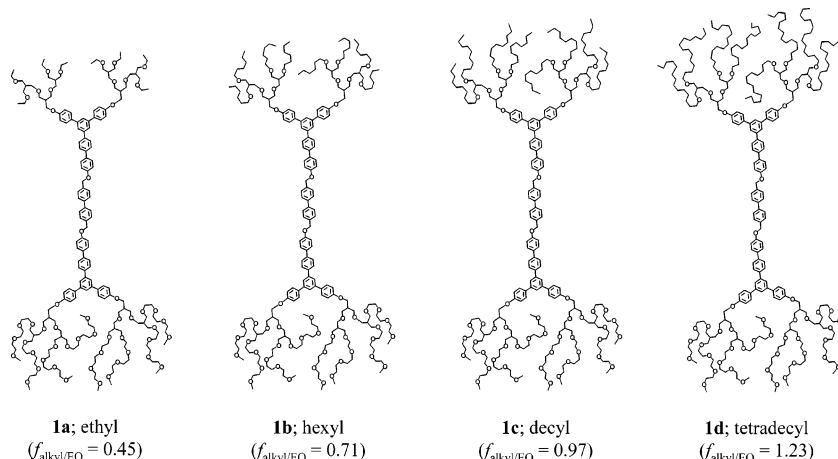
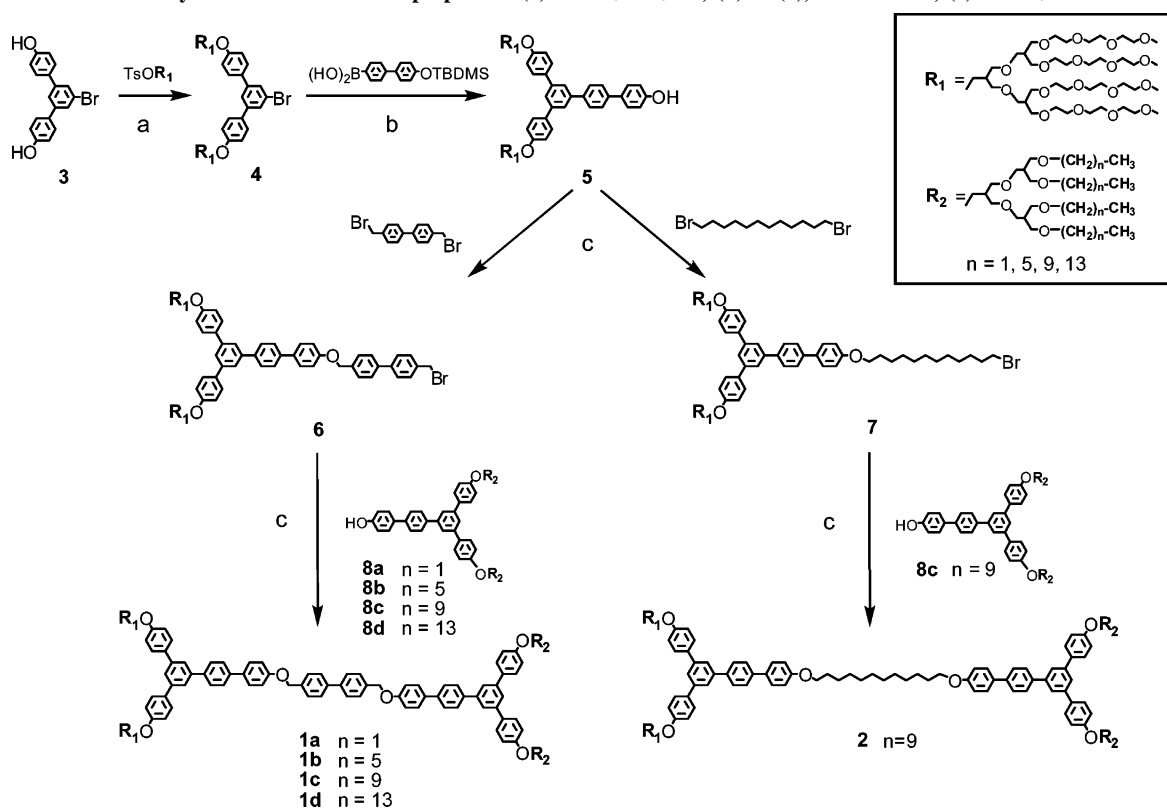
ular dumbbells which can self-assemble into unique 2-D supramolecular structures due to enhanced hydrophobic interactions and subsequent space filling requirements. Indeed, asymmetric dumbbell-shaped rod amphiphiles in aqueous solution showed to self-assemble successively into spherical, toroidal, and cylindrical micelles, as the hydrophobic alkyl chains of the molecules increase in length relative to the hydrophilic dendron segments.⁸ More recently, we have also shown that rod amphiphilic molecules containing hydrophilic dendrons at one end and hydrophobic ones at the other end can generate 2-D networks and closed sheets depending on the rod length.⁹ This result indicates that increasing the rod length directs the planar nets toward the closed 2-D structure through increasing π -stacking interactions. This stimulates us to envision that systematic variation in the relative volume fraction of hydrophobic branched chains to hydrophilic dendrons can give rise to the successive structural progression including unusual intermediate structures such as toroids and 2-D nets in a homologous series. In this context, we have synthesized a series of asymmetric dumbbell-shaped rod amphiphiles based on hydrophilic oligoether dendrons at one end and hydrophobic branched alkyl chains at the other end of the rod segment with systematic variation in the alkyl length from ethyl to tetradecyl group (Chart 1).

Results and Discussion

Synthesis. The synthesis of amphiphilic dumbbell-shaped molecules consisting of a rod segment connected by hydrophilic oligoether dendrons at one end and hydrophobic branched alkyl chains at the other end is outlined in Scheme 1 and started with the preparation of dendritic oligoether dendrons and branched alkyl chains according to the procedures described previously.^{10–12}

* Corresponding author. Prof. Myongsoo Lee, Center for Supramolecular Nano-Assembly and Department of Chemistry, Yonsei University, Shinchon 134, Seoul 120-749, Korea. Phone: 82-2-2123-2647. Fax: 82-2-393-6096. E-mail: mslee@yonsei.ac.kr.

Chart 1. Chemical Structure of Asymmetric Dumbbell-Shaped Rod Amphiphiles 1a–1d

Scheme 1. Synthesis of the Rod Amphiphiles: (a) $\text{K}_2\text{CO}_3/\text{CH}_3\text{CN}$; (b) $\text{Pd}(0)$, NaOH/THF ; (c) $\text{K}_2\text{CO}_3/\text{Acetone}$.

The design of a hydrophilic dendritic flexible chain was focused on the construction of an oligo(ethylene oxide) dendritic segment that is readily soluble in water. The meta-linked dihydroxy triphenylene derivative (**3**) was prepared according to the procedures described previously,^{11,12} and then the subsequent etherification with tosylated oligoether dedron yielded **4**, showing sufficient solubility for further coupling of rigid conjugated building blocks in the reaction medium. **5** was prepared from the Suzuki coupling reaction with **4** and 4-(*tert*-butyldimethylsilyloxy)-biphenyl-4'-boronic acid in the presence of $\text{Pd}(0)$ catalysis.^{11–13} Similarly, the Y-shaped rigid aromatic segments **8a–8d** with appropriate hydrophobic alkyl dendrons were synthesized using the same procedure. The synthesis of **8a–8d** were performed according to the procedure used for **5**. The precursor of the rod amphiphiles (**6**) was synthesized by an etherification reaction of **5** with 4,4'-bis(bromomethyl)-biphenyl in the presence of potassium carbonate. Etherification

of **6** with an excess of **8a–8d** produced the final dumbbell-shaped rod amphiphiles **1a–1d**, respectively. For comparative study, an amphiphilic molecule with a lack of an extended rod segment (**2**) was prepared by the same sequence of reactions, i.e., by etherification of **5** with an excess of 1,12-dibromododecane and subsequent etherification with **8c**. The resulting amphiphilic molecules were characterized by ^1H NMR spectroscopy, elemental analysis, and MALDI-TOF mass spectrometry and were shown to be in full agreement with the expected chemical structures.

The molecular dumbbells, when dissolved in a solvent suitable for the oligoether segments, can self-assemble into an aggregation structure because of their amphiphilic characteristics.¹⁴ Aggregation behavior of the molecules was subsequently studied in aqueous solution by using transmission electron microscopy (TEM). In an effort to provide direct visualization of the aggregate structures formed in water without artifacts, cryogenic-

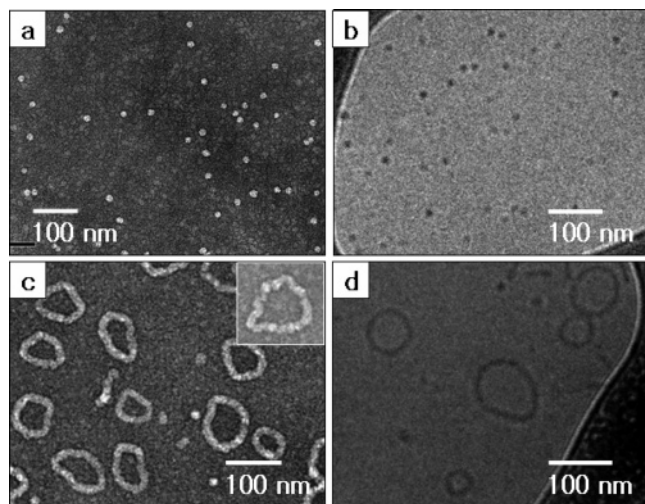


Figure 1. Aggregation behavior of the rod amphiphiles in aqueous solution (0.01 wt %) at room temperature. (a) TEM image of a cast film (stained with uranyl acetate), and (b) cryo-TEM image exhibiting a spherical structure of **1a**. (c) TEM image of a cast film (inset, image of a nanoring with undulations), and (d) cryo-TEM image showing a toroidal structure of **1b**.

transmission electron microscopy (cryo-TEM) investigations were performed with the dumbbell-shaped amphiphiles in aqueous solution.¹⁵

1a based on an ethyl group, which is the smallest relative volume fraction of hydrophobic branched chains to oligoether dendrons ($f_{\text{alkyl/EO}} = 0.45$), showed to self-assemble into discrete spherical objects with a uniform size (Figure 1a). The cryo-TEM image revealed the presence of spherical aggregates with an average diameter of 11 nm against the vitrified solution background (Figure 1b). The hydrophobic cores appeared to be dark, whereas the solvated oligoether dendrons were not directly visible.¹⁶ Thus, these dimensions of the diameter of aggregates correspond to approximately twice the extended hydrophobic segments (~ 5.6 nm by CPK modeling), including the rod and alkyl chains, implying that aggregates of **1a** are close to micellar in nature.

Notably, an increase in the alkyl chain from ethyl to hexyl ($f_{\text{alkyl/EO}} = 0.71$) gives rise to a significant structural change from spheres to toroids. When the sample was cast from a 0.01 wt % solution of **1b** and then negatively stained with uranyl acetate, the images showed predominantly ring-shaped micelles together with a few discrete spherical and cylindrical micelles (Figure 1c). The cross-sectional diameter of the rings is 15 nm, and the ring size diameters range from 60 to 250 nm, which gives an average value of ~ 115 nm. To directly substantiate the formation of toroids, cryo-TEM experiments were performed with a 0.01 wt % solution of **1b**. Figure 1d clearly shows dark toroidal objects with a uniform diameter of ~ 12 nm, indicating that the solvent evaporation process on the TEM grid does not have any noticeable influence on the aggregation structure. It should be noted that the observed diameter is smaller than the result obtained from the cast film. This could be attributed to low contrast of the hydrated oligoether dendrons.¹⁶ The dimension of 12 nm is in reasonable agreement with twice the length of the hydrophobic segments, including the rod and alkyl chains. Considering this cross-sectional diameter, the inner core of the ring consists of a hydrophobic rod and alkyl chains surrounded by hydrophilic ethylene oxide dendrons. Closer examination of a toroid revealed that some rings are composed of undulations in the cross-section, suggesting that the rings are formed through coalescence of

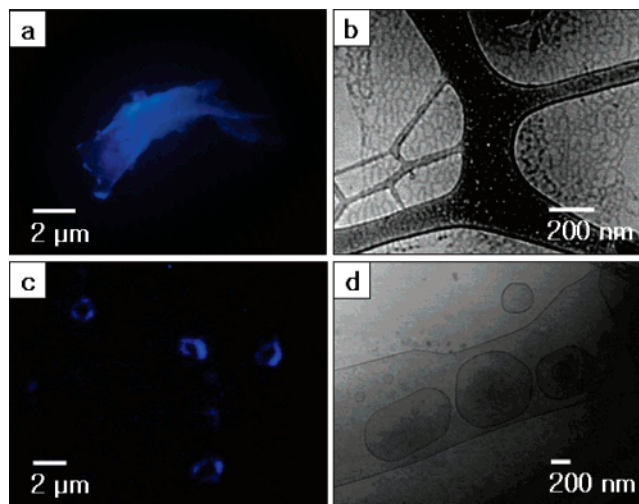


Figure 2. (a) Fluorescence micrograph in aqueous solution of **1c**. (b) Cryo-TEM image of a planar network structure formed from **1c**. (c) Fluorescence micrograph in aqueous solution of **1d**. (d) Cryo-TEM image of vesicles formed from **1d**.

spherical objects (Figure 1c, inset). The tendency of spherical micelles to transform into a toroidal structure on increasing the volume fraction of hydrophobic alkyl chains is consistent with the results observed in our laboratory.⁸

A further increase in the length of the alkyl chain to a decyl group drives the system to form 2-D sheets. This was confirmed by fluorescence and cryo-TEM investigations with a 0.01 wt % aqueous solution of **1c** ($f_{\text{alkyl/EO}} = 0.97$). The fluorescence microscopy image revealed the presence of flat sheets (Figure 2a). The magnification of the 2-D objects by cryo-TEM showed that the sheets consist of in-plane nanopores, consistent with the result reported previously.^{9,17} These results imply that the toroidal structure is possible to transform directly into planar nets without passing through an intermediate structure such as extended cylindrical micelles, which will be discussed later.

In great contrast to **1c**, **1d** with the longest alkyl groups ($f_{\text{alkyl/EO}} = 1.23$) exhibits a hollow vesicular structure. A fluorescence image of a **1d** solution (0.01 wt %) revealed the formation of giant spherical objects with dark inside, characteristic of hollow spherical objects.¹⁸ To provide further evidence for the formation of a vesicular structure, cryo-TEM experiments were carried out with a 0.01 wt % solution of **1d** (Figure 2d). The image showed a closed vesicular structure with diameters ranging from several hundred nanometers to a few micrometers and a uniform bilayer thickness of 13 nm. This result indicates that an increase in the hydrophobic alkyl length decreases interfacial curvature to relieve the energetic penalty associated with loosely packed edge parts.¹⁹ Consequently, the 2-D nets with in-plane nanopores transform into a hollow vesicular structure to avoid energetically unfavorable edges.

The results described here demonstrate that, as the chain length of the hydrophobic alkyl group in the amphiphilic molecule increases, the self-assembled structure successively changes from closed spheres, toroids, 2-D nets, to vesicles. This progression of aggregate structures formed from the aqueous self-assembly of the rod amphiphiles can be explained in terms of the energy balance between repulsive interactions among the oligoether dendrons and attractive hydrophobic interactions including π -stacking forces of the rod segments (Figure 3).²⁰ The rod amphiphile with short alkyl chains self-assembles into closed spherical micelles in which the rod segments may pack

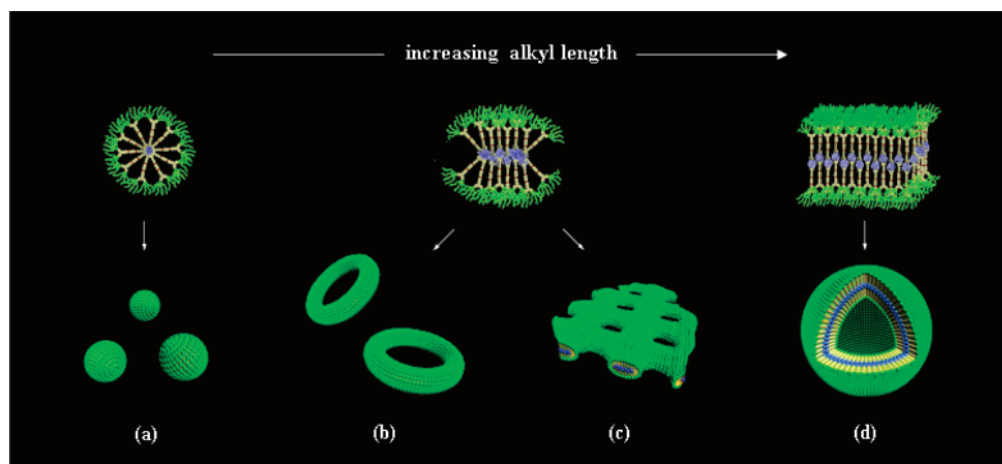


Figure 3. Schematic illustration for molecular organization of the dumbbell-shaped rod amphiphiles and subsequent formation of supramolecular structures from (a) spheres, (b) toroids, (c) 2-D nets, and (d) vesicles with increasing the length of alkyl chain.

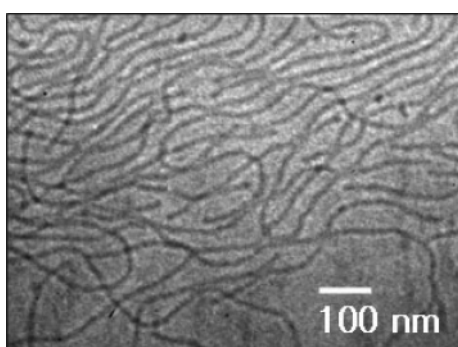


Figure 4. Cryo-TEM image of the long cylindrical structure of **2**.

with a more radial arrangement to avoid contact between hydrophobic side faces of the rod amphiphiles and water. On increasing the length of the alkyl chain, hydrophobic interactions would be greater to enforce the rod segments to align with a more parallel arrangement to reduce steric problems for close packing. Subsequently, the spherical micelles coalesce into larger aggregates in a two-dimensional way to increase the extent of parallel packing of the rod segments with a simultaneous decrease in unfavorable contact between hydrophobic segments and water molecules. The increment in the extent of parallel arrangement at the expense of radial arrangement is reflected in the systematic shift of the absorption edge toward higher wavelengths in UV-vis absorption spectra, indicating that π -stacking interactions between adjacent rod segments increase with increasing the alkyl length.²¹ As a result, the strong propensity of the elongated rod segments to be aligned in a parallel fashion, together with repulsive interactions of bulky oligoether dendrons, seems to be the primary driving forces in this structural progression.

To gain insight into the role of the elongated rod segments for the 2-D assembly, we have replaced the central biphenyl unit of **1c** into an aliphatic dodecyl group to form a flexible analogue (**2**) to **1c** with the aim of disruption of π -stacking anisotropic interactions. In great contrast to the rod amphiphile, **2** showed to form extended cylindrical micelles with a uniform diameter in aqueous solution under standard conditions (Figure 4). It is well-known that cylindrical micelles exist as an intermediate structure between spherical micelles and vesicles in coil-coil block copolymers and low molecular weight surfactant solutions.²² Therefore, this result implies that the formation of toroids and planar nets from the rod amphiphiles as intermediate phases between spheres and vesicles originates

from the anisotropic arrangement of the conformationally stiff rod segments.

Another interesting point to be noted is that the aggregate structures consist of a hydrophilic ethylene oxide dendritic exterior which is well-known to exhibit a lower critical solution temperature (LCST) behavior in aqueous media.^{23,24} Above the LCST, the ethylene oxide segments are dehydrated to collapse into molecular globules. Consequently, a significant structural transformation can be expected to happen by changing temperature. Accordingly, temperature responsive solution behavior was investigated with **1b** by means of UV-vis transmittance. The turbidity measurements showed the LCST transition to be 50 °C (Figure 5a), at which dehydration of the ethylene oxide chains occurs to collapse into molecular globules. This dehydration was further confirmed by ¹H NMR measurements. The resonances associated with the ethylene oxide chains showed to be broadened together with a decrease in intensity (Figure 5b) upon heating above the LCST, clearly demonstrating the loss of hydrogen bonding interactions between ether oxygens and water molecules.²⁴ To corroborate structural change at the LCST, cryo-TEM was carried out with **1b** as a function of temperature. When the temperature was raised to 50 °C, the micrograph showed fused toroids and fragmented networks with irregular pores (Figure 5c). On further heating to 70 °C, these small 2-D fragments are coalesced into large planar sheets with in-plane nanopores with diameters ranging from 15 to 110 nm (Figure 5d). The planar nets showed to be recovered into a toroidal structure when cooling to room temperature, indicating that this phase transition is reversible on heating and cooling cycles. This result demonstrates that the toroidal structure of **1b** transforms directly into the planar nets in a reversible way by changing temperature.

This structural transition can be explained because the oligo-(ethylene oxide) dendrons located at the exterior of toroids shrink with increasing temperature caused by LCST phase behavior, as evidenced by turbidity and ¹H NMR measurements. Consequently, the rod segments, upon heating, are packed more closely in a parallel fashion within the toroidal core due to shrinkage of the oligoether dendritic segments caused by dehydration, again resulting in the exposure of the hydrophobic side faces to water. To reduce this unfavorable contact, the toroids are fused together through side by side hydrophobic interactions to form 2-D nets (Figure 6). Therefore, the temperature effect is a similar way to how the 2-D structure is formed in preference to toroids with increasing the volume fraction of hydrophobic alkyl chains, as discussed earlier.

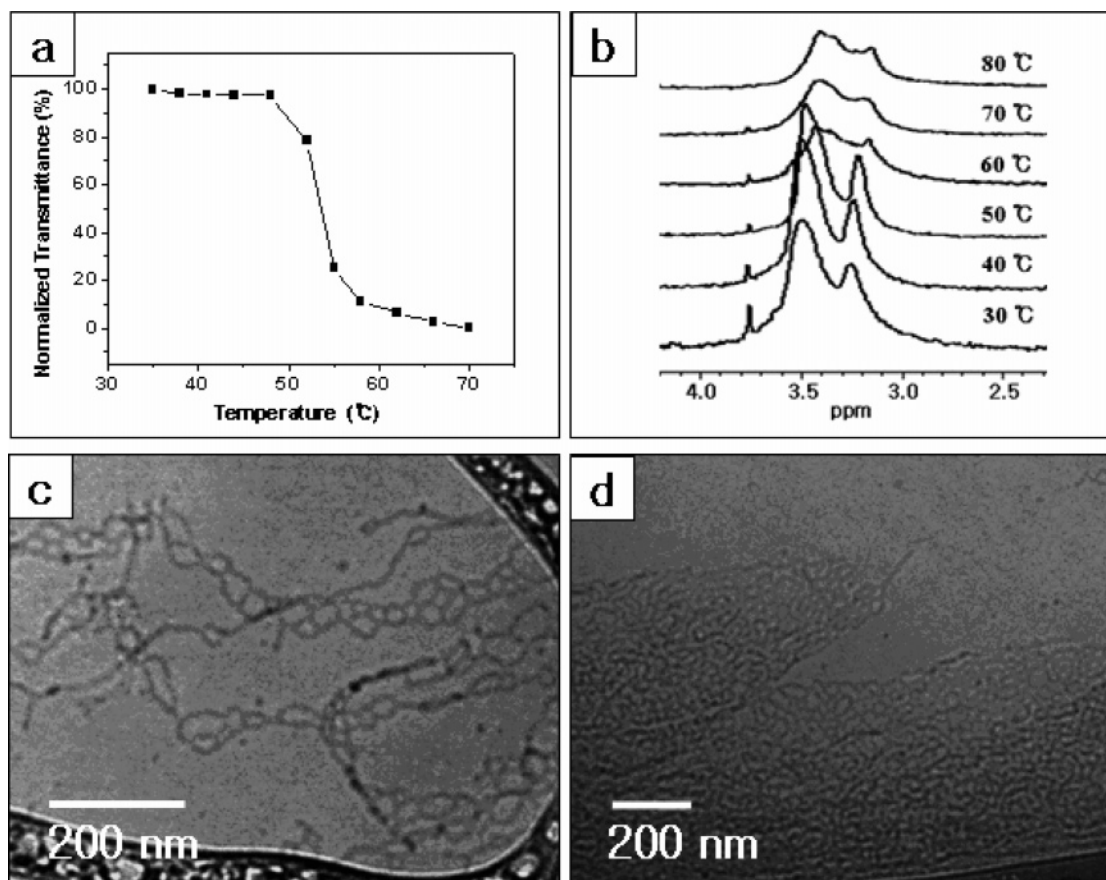


Figure 5. (a) Optical transmittance of aqueous solution of **1b** upon heating at various temperatures. (b) ^1H NMR spectra of ethylene oxide regions of **1b** (400 MHz) in D_2O (0.03 wt %) and used 1,4-dioxane as an internal standard. Cryo-TEM images of aqueous solution of **1b** (c) at 50 °C and (d) 70 °C.

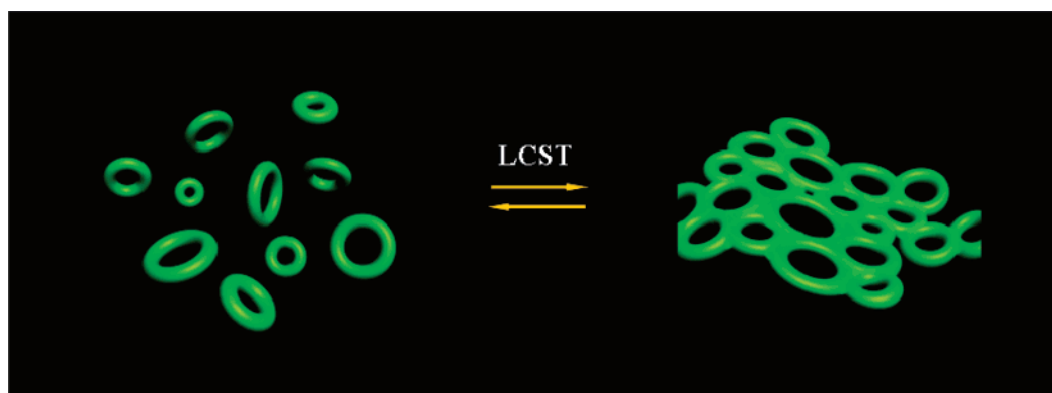


Figure 6. Schematic representation of reversible transformation from toroids to 2-D nets.

Conclusions

The results described here demonstrate that as the hydrophobic alkyl chain length of the asymmetric rod amphiphile increases, the self-assembled structure changes significantly from closed spheres, to toroids, then to planar nets, and finally to vesicles. This complicated structural transformation seems to originate from a consequence of the delicate balance between the repulsive interactions of the oligoether dendrons and attractive π -stacking interactions of the rod segments. Considering that the conventional self-assembling systems such as coil-coil block copolymer and surfactant molecules form branched cylinders or 3-D networks as an intermediate structure,²⁵ the unique feature of the rod amphiphiles investigated here is their ability to self-assemble into unusual toroidal and 2-D network structures as intermediate phases between sphere and vesicles.

Remarkably, the structural change from toroids to planar nets was also accompanied by temperature variation as in the case of **1b**. Therefore, changing temperature produces an effect similar to varying the relative volume fraction of the hydrophilic ethylene oxide chains. It should be noted that this structural change takes place directly without passing through an intermediate structure such as extended cylindrical micelles. This direct structural transition can be rationalized by considering a LCST behavior of the oligoether dendrons that results in the change of the relative extent of parallel arrangements of the rod segments to that of radial arrangement at the rod segments.

This work demonstrates a strategy of controlling supramolecular nanostructures of the rod amphiphiles in an aqueous medium by only a small variation in the length of grafted alkyl chains. In an effort to expand potential applications for

functional materials, the results described here provide a first step toward tunable nanoscopic properties in aqueous media.

Acknowledgment. This work was supported by the National Creative Research Initiative Program of the Korean Ministry of Science and Technology. E.L. thanks the Seoul Science Fellowship Program, and E.L., Y.-H.J. and J.-K.K. acknowledge a fellowship of the BK21 program from the Ministry of Education and Human Resources Development.

Supporting Information Available: Synthetic and other experimental details. This material is available free of charge via the Internet at <http://pubs.acs.org>.

References and Notes

- (1) (a) Lehn, J.-M. *Proc. Natl. Acad. Sci. U.S.A.* **2002**, *99*, 4763–4768. (b) Lee, M.; Cho, B.-K.; Zin, W.-C. *Chem. Rev.* **2001**, *101*, 3869–3892. (c) Sarikaya, M.; Tamerler, C.; Jen, A. K.-Y.; Schulten, K.; Baneyx, F. *Nature Mater.* **2003**, *2*, 577–585. (d) Hoeben, F. J. M.; Jonkheijm, P.; Meijer, E. W.; Schenning, A. P. H. J. *Chem. Rev.* **2005**, *105*, 1491–1546. (e) Cornelissen, J. J. L. M.; Rowan, A. E.; Nolte, R. J. M.; Sommerdijk, N. A. J. M. *Chem. Rev.* **2001**, *101*, 4039–4070.
- (2) (a) Das, G.; Ouali, L.; Adrian, M.; Baumeister, B.; Wilkinson, K. J.; Matile, S. *Angew. Chem., Int. Ed.* **2001**, *40*, 4657–4661. (b) Yang, W.-Y.; Lee, E.; Lee, M. *J. Am. Chem. Soc.* **2006**, *128*, 3484–3485. (c) Zubarev, E. R.; Pralle, M. U.; Sone, E. D.; Stupp, S. I. *J. Am. Chem. Soc.* **2001**, *123*, 4105–4106. (d) Hill, J. P.; Jin, W.; Kosaka, A.; Fukushima, T.; Ichihara, H.; Shimomura, T.; Ito, K.; Hashizume, T.; Ishii, N.; Aida, T. *Science* **2004**, *304*, 1481–1483. (e) Vriezema, D. M.; Hoogboom, J.; Velonia, K.; Takazawa, K.; Christianen, P. C. M.; Maan, J. C.; Rowan, A. E.; Nolte, R. J. M. *Angew. Chem., Int. Ed.* **2003**, *42*, 772–776. (f) Yoo, Y.-S.; Choi, J.-H.; Song, J.-H.; Oh, N.-K.; Zin, W.-C.; Park, S.; Chang, T.; Lee, M. *J. Am. Chem. Soc.* **2004**, *126*, 6294–6300.
- (3) (a) Horsch, M. A.; Zhang, Z.; Glotzer, S. C. *Nano Lett.* **2006**, *6*, 2406–2413. (b) Chen, Z.; Cui, H.; Hales, K.; Li, Z.; Qi, K.; Pochan, D. J.; Wooley, K. L. *J. Am. Chem. Soc.* **2005**, *127*, 8592–8593. (c) van Hest, J. C. M.; Delnoye, D. A. P.; Baars, M. W. P. L.; van Genderen, M. H. P.; Meijer, E. W. *Science* **1995**, *268*, 1592–1595. (d) Cornelissen, J. J. L. M.; Fischer, M.; Sommerdijk, N. A. J. M.; Nolte, R. J. M. *Science* **1998**, *280*, 1427–1430.
- (4) (a) Ryu, J.-H.; Lee, M. *J. Am. Chem. Soc.* **2005**, *127*, 14170–14171. (b) Schenning, A. P. H. J.; Kilbinger, A. F. M.; Biscarini, F.; Cavallini, M.; Cooper, H. J.; Derrick, P. J.; Feast, W. J.; Lazzaroni, R.; Leclere, Ph.; McDonnell, L. A.; Meijer, E. W.; Meskers, S. C. J. *J. Am. Chem. Soc.* **2002**, *124*, 1269–1275.
- (5) Henze, O.; Feast, W. J.; Gardebien, F.; Jonkheijm, P.; Lazzaroni, R.; Leclere, Ph.; Meijer, E. W.; Schenning, A. P. H. J. *J. Am. Chem. Soc.* **2006**, *128*, 5923–5929.
- (6) Bae, J.; Choi, J.-H.; Yoo, Y.-S.; Oh, N.-K.; Kim, B.-S.; Lee, M. *J. Am. Chem. Soc.* **2005**, *127*, 9668–9669.
- (7) Ryu, J.-H.; Kim, H.-J.; Huang, Z.; Lee, E.; Lee, M. *Angew. Chem., Int. Ed.* **2006**, *45*, 5304–5307.
- (8) Kim, J.-K.; Lee, E.; Huang, Z.; Lee, M. *J. Am. Chem. Soc.* **2006**, *128*, 14022–14023.
- (9) Kim, J.-K.; Lee, E.; Jeong, Y.-H.; Lee, J.-K.; Zin, W.-C.; Lee, M. *J. Am. Chem. Soc.* **2007**, *129*, 6082–6083.
- (10) Jayaraman, M.; Fréchet, J. M. J. *J. Am. Chem. Soc.* **1998**, *120*, 12996–12997.
- (11) Ryu, J.-H.; Oh, N.-K.; Lee, M. *Chem. Commun.* **2005**, 1770–1772.
- (12) Jang, C.-J.; Ryu, J.-H.; Lee, J.-D.; Sohn, D.; Lee, M. *Chem. Mater.* **2004**, *16*, 4226–4231.
- (13) Ryu, J.-H.; Bae, J.; Lee, M. *Macromolecules* **2005**, *38*, 2050–2052.
- (14) Förster, S.; Plantenberg, T. *Angew. Chem., Int. Ed.* **2002**, *41*, 688–714.
- (15) (a) Dan, N.; Shimon, K.; Pata, V.; Danino, D. *Langmuir* **2006**, *22*, 9860–9865. (b) Battaglia, G.; Ryan, A. J. *J. Am. Chem. Soc.* **2005**, *127*, 8757–8764.
- (16) (a) Zheng, Y.; Won, Y.-Y.; Bates, F. S.; Davis, H. T.; Scriven, L. E.; Talmon, Y. *J. Phys. Chem. B* **1999**, *103*, 10331–10334. (b) Mortensen, K.; Talmon, Y.; Gao, B.; Kops, J. *Macromolecules* **1997**, *30*, 6764–6770. (c) Li, Z.; Kesselman, E.; Talmon, Y.; Hillmyer, M. A.; Lodge, T. P. *Science* **2004**, *306*, 98–101.
- (17) These nanostructures were essentially unchanged with concentration in the range from 0.01 to 0.1 wt % (see Supporting Information).
- (18) (a) Bellomo, E. G.; Wyrsta, M. D.; Pakstis, L.; Pochan, D. J. *Nature Mater.* **2004**, *3*, 244–248. (b) Holowka, E. P.; Pochan, D. J.; Deming, T. J. *J. Am. Chem. Soc.* **2005**, *127*, 12423–12428. (c) Han, M.; Hara, M. *J. Am. Chem. Soc.* **2005**, *127*, 10951–10955.
- (19) (a) Shioi, A.; Hatton, T. A. *Langmuir* **2002**, *18*, 7341–7348. (b) Li, Z.; Hillmyer, M. A.; Lodge, T. P. *Nano Lett.* **2006**, *6*, 1245–1249. (c) Weiss, T. M.; Narayanan, T.; Wolf, C.; Gradzielski, M.; Panine, P.; Finet, S.; Hellsby, W. I. *Phys. Rev. Lett.* **2005**, *94*, 038303-1.
- (20) (a) Williams, D. R. M.; Fredrickson, G. H. *Macromolecules* **1992**, *25*, 3561–3568. (b) Horsch, M. A.; Zhang, Z.; Glotzer, S. C. *Phys. Rev. Lett.* **2005**, *95*, 056105-1. (c) Halperin, A. *Macromolecules* **1990**, *23*, 2724–2731.
- (21) (a) McQuade, D. T.; Kim, J.; Swager, T. M. *J. Am. Chem. Soc.* **2000**, *122*, 5885–5886. (b) Jonkheijm, P.; Hoeben, F. J. M.; Kleppinger, R.; van Herikhuyzen, J.; Schenning, A. P. H. J.; Meijer, E. W. *J. Am. Chem. Soc.* **2003**, *125*, 15941–15949. (c) Lee, M.; Jeong, Y.-S.; Cho, B.-K.; Oh, N.-K.; Zin, W.-C. *Chem.—Eur. J.* **2002**, *8*, 876–883.
- (22) (a) Zupancich, J. A.; Bates, F. S.; Hillmyer, M. A. *Macromolecules* **2006**, *39*, 4286–4288. (b) Zhang, L.; Eisenberg, A. *Science* **1995**, *268*, 1728–1731. (c) He, Y.; Li, Z.; Simone, P.; Lodge, T. P. *J. Am. Chem. Soc.* **2006**, *128*, 2745–2750. (d) Israelachvili, J. N. *Intermolecular and Surface Forces*; Academic Press: New York, 1985.
- (23) (a) Smith, G. D.; Bedrov, D. *J. Phys. Chem. B* **2003**, *107*, 3095–3097. (b) Aathimanikandan, S. V.; Savariar, E. N.; Thayumanavan, S. *J. Am. Chem. Soc.* **2005**, *127*, 14922–14929. (c) Dormidontova, E. E. *Macromolecules* **2002**, *35*, 987–1001. (d) Jia, Z.; Chen, H.; Zhu, X.; Yan, D. *J. Am. Chem. Soc.* **2006**, *128*, 8144–8145.
- (24) (a) Hua, F.; Jiang, X.; Zhao, B. *Macromolecules* **2006**, *39*, 3476–3479. (b) Zhou, Y.; Yan, D.; Dong, W.; Tian, Y. *J. Phys. Chem. B* **2007**, *111*, 1262–1270.
- (25) (a) Jain, S.; Bates, F. S. *Science* **2003**, *300*, 460–464. (b) Bernheim-Groswasser, A.; Wachtel, E.; Talmon, Y. *Langmuir* **2000**, *16*, 4131–4140.

MA071511+